Materials Advances

ROYAL SOCIETY OF CHEMISTRY

PAPER

View Article Online
View Journal | View Issue

Cite this: *Mater. Adv.*, 2022, 3, 5813

Photoinduced degradation of thermally stable $Cs_2AgBiBr_6$ double perovskites by micro-Raman studies†

Athrey C. Dakshinamurthy and C. Sudakar *

Received 16th February 2022,
Accepted 24th May 2022

DOI: 10.1039/d2ma00179a

rsc.li/materials-advances

The thermal stability of lead-free double perovskite $Cs_2AgBiBr_6$ for stable optoelectronic and photovoltaic devices is essential. There are contradicting reports, with some claiming stability from 300 to 400 °C based on X-ray diffraction and thermogravimetry studies and others up to 250 °C from Raman studies for $Cs_2AgBiBr_6$. We perform thermogravimetry analysis and temperature-dependent Raman studies with different laser intensities and show that $Cs_2AgBiBr_6$ is thermally stable up to ~410 °C. A low power (3.68 mW) laser excitation source does not induce any structural changes at all temperatures. On the contrary, higher power laser light (7.15 mW) decomposes $Cs_2AgBiBr_6$ to $Cs_3Bi_2Br_9$ at temperatures beyond 180 °C. Meticulous thermogravimetry, Raman, and X-ray diffraction studies confirm that $Cs_2AgBiBr_6$ is structurally stable up to 410 °C, whereas its stability decreases under light exposure beyond a certain critical intensity. This study brings out the importance of light and thermal stability of $Cs_2AgBiBr_6$, which is crucial for designing various optoelectronic devices.

1. Introduction

Halide double perovskites (HDPs) of the form $A_2B'B''X_6$ are emerging as a promising alternative to lead-based inorganic perovskites due to their efficiency and promising applications in photovoltaics and optoelectronics.[1,2] HDPs exhibit exceptional thermal stability and nontoxicity in addition to their promising optical properties.[1] In HDPs, B′ and B″ are monovalent and trivalent metal cations, thus forming a three-dimensional network of corner-connected metal-halide octahedra. Among various HDPs, $Cs_2AgBiBr_6$ is gaining significant momentum due to its reduced band gap (~1.7–2.1 eV), long carrier lifetimes (> 1 μs), and smaller carrier effective mass, making it a promising candidate for photovoltaic and photocatalytic devices.[3–6] Solar cells with $Cs_2AgBiBr_6$ as photo-absorbers have been fabricated recently, which show a promising efficiency of over 3%.[7] Nevertheless, studies on the stability of double perovskites or degradation under thermal and photoinduced conditions are scarce in the literature. Burwig *et al.* have demonstrated through X-ray diffraction studies that the annealing temperature plays a crucial role in the phase and crystal structure evolution in $Cs_2AgBiBr_6$, with the cubic phase shown to be stable up to 300 °C.[8] Beyond this temperature, it was ambiguous whether a high-temperature $Cs_2AgBiBr_6$ phase is formed, or thermal degradation begins. Contrastingly, Pistor *et al.* have reported that the $Cs_2AgBiBr_6$ undergoes thermal decomposition to $Cs_3Bi_2Br_9$ at 250 °C.[9] In fact, recent studies on solar cells fabricated using a $Cs_2AgBiBr_6$ absorber layer, reported by Ghasemi *et al.*, demonstrated that the dual ion diffusion (Ag^+ and Br^-) of the material, which is an intrinsic property, affects the long term operational stability of the device.[10] Thus, there is a lack of understanding of the structural stability and phase stability of $Cs_2AgBiBr_6$ double perovskites at elevated temperatures.

Laser irradiation is widely used to probe various structural, vibrational, and optical properties. However, stability or degradation studies of HDPs under laser light exposure are scarce. Thermally-induced phase changes and compositional modification due to chemical effects caused by such exposure need to be understood. Various photochemical transformations such as oxidation-reduction, defect formation, phase transitions, and laser-induced degradation occur upon laser exposure.[11,12] Such changes are mostly observed in lead-halide perovskites.[12] Although HDPs are mostly known to be stable under ambient conditions and light exposure, it is important to explore the laser-induced effects as these compounds show applicability in high-energy X-ray and UV radiation detectors.[13,14]

In this communication, we demonstrate that the $Cs_2AgBiBr_6$ compound is thermally stable up to ~410 °C, in contrast to an earlier observation[9] that $Cs_2AgBiBr_6$ degrades to $Cs_3Bi_2Br_9$ at 250 °C. We unequivocally show, on the other hand, that $Cs_2AgBiBr_6$ degrades to the $Cs_3Bi_2Br_9$ phase even at 180 °C only

Multifunctional Materials Laboratory, Department of Physics, Indian Institute of Technology Madras, Chennai, 600036, India. E-mail: csudakar@iitm.ac.in

† Electronic supplementary information (ESI) available. See DOI: https://doi.org/10.1039/d2ma00179a

upon exposure to a high intense laser power of ~7.15 mW, revealing the instability of $Cs_2AgBiBr_6$ under intense photon interaction.

2. Experimental details

$Cs_2AgBiBr_6$ double perovskite powder is synthesized through a modified solution-based approach reported earlier.[15] In a typical synthesis, stoichiometric concentrations of bismuth acetate and silver acetate are dissolved in HBr solution at 170 °C. After complete dissolution, CsBr is added to the above precursor solution. At this point, an orange-red precipitate immediately forms, indicating the crystallization and growth of $Cs_2AgBiBr_6$. The precipitate is filtered and dried at 75 °C. The crystal structure and phase purity of $Cs_2AgBiBr_6$ are analyzed by powder X-ray diffractometry (Rigaku SmartLab) with a CuKα (λ = 1.5406 Å) X-ray source. The Raman spectra are acquired using a Horiba-JobinYvon (HR 800 UV) micro-Raman spectrometer operating with a 632 nm laser excitation source. Raman spectra are also acquired at various temperatures with a Linkam stage attached to the spectrometer in a backscattered configuration with the microscope. Differential scanning calorimetry (DSC) and thermogravimetric analysis (TGA) are simultaneously performed using a DSC-TGA Standard, SDT Q600 V20.9 Build 20 instrument to evaluate thermal stability and phase changes such as decomposition of $Cs_2AgBiBr_6$.

3. Results and discussion

X-Ray diffraction (XRD) studies show that the synthesized compound exhibits phase pure composition of $Cs_2AgBiBr_6$ without the presence of any trace of other secondary phases (Fig. 1). $Cs_2AgBiBr_6$ crystallizes into a cubic elpasolite structure with the space group $Fm\bar{3}m$ symmetry. Ag^+ and Bi^{3+} exhibit rock salt ordering in the structure, as evident from the presence of all odd Miller indices in the XRD pattern. The lattice parameter estimated using Rietveld refinement gives a = 11.2719 Å, which matches with the reported values.

Raman spectral analyses are performed on $Cs_2AgBiBr_6$ to elucidate the local structural information using octahedral vibrational modes and the stability of the compound as a function of temperature. Fig. 2 shows the Raman spectra of the $Cs_2AgBiBr_6$ compound at various temperatures in the range from 30 °C to 310 °C performed using 3.68 mW and 7.15 mW laser power of a 632 nm excitation source, which corresponds to a power density of ~1.1 mW μm^{-2} and 2.2 mW μm^{-2}, respectively. The beam size of the laser is ~2 μm in all these measurements. Based on the Wyckoff positions of atoms and symmetry considerations, four modes *viz.*, F_{2g} (2 modes), E_g, and A_{1g} are Raman active in $Cs_2AgBiBr_6$. These modes are attributed to the scissoring motion of Br atoms along with Cs motion, and asymmetric and symmetric stretching of $[AgBr_6]^{5-}$ octahedra, respectively.[16] The vibrational energies of these modes observed at 30 °C are in good agreement with the values reported in the literature.[9]

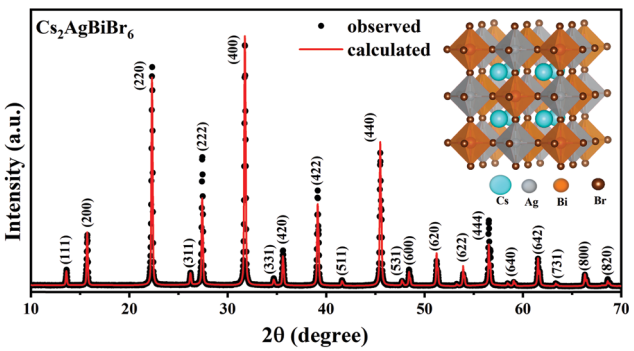

Fig. 1 Powder XRD pattern of the synthesized $Cs_2AgBiBr_6$ along with the Rietveld refinement. Inset shows its crystal structure.

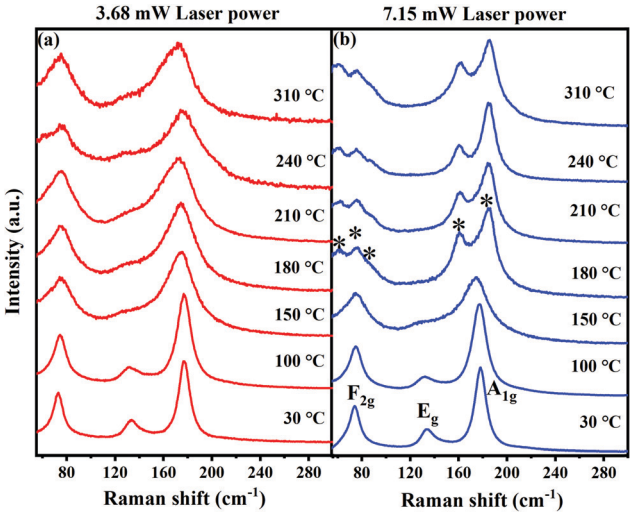

Fig. 2 Raman spectra of $Cs_2AgBiBr_6$ acquired at various temperatures using a 632 nm He–Ne-ion laser with (a) 3.68 mW and (b) 7.15 mW laser power.

The temperature stability of the $Cs_2AgBiBr_6$ and laser-induced effects on the structure can be directly inferred from the Raman spectra acquired at different temperatures using two different laser powers. When excited with lower laser power (~3.68 mW), all the Raman modes are clearly discernible at all the temperatures suggesting the robust structural stability of $Cs_2AgBiBr_6$. The vibrational modes get substantially broadened with an increase in temperature due to the increased anharmonicities in the atomic vibrations at elevated temperatures. Most importantly, the cubic structure of $Cs_2AgBiBr_6$ is retained at high temperatures indicating that the compound $Cs_2AgBiBr_6$ is highly stable and does not undergo any thermal degradation. This agrees well with the studies reported by Burwig *et al.*, where they demonstrated through XRD measurements that the $Cs_2AgBiBr_6$ structure is stable up to 300 °C and can be clearly assigned to the cubic polymorph.[8] In their report, it is quite ambiguous, for temperatures greater than 300 °C, whether $Cs_2AgBiBr_6$ remains still in a cubic structure or undergoes phase degradation. However, a recent report by Pistor *et al.* showed contrastingly different results, wherein they demonstrated that the cubic structure of $Cs_2AgBiBr_6$ undergoes

thermally induced phase degradation to a layered $Cs_3Bi_2Br_9$ structure at 250 °C.[9] This has been inferred from the changes observed in the Raman spectra acquired after annealing the samples at various temperatures. In fact, we observe a similar feature; however, when the Raman spectra are acquired with a higher laser power (7.15 mW), as shown in Fig. 2b.

Halide single perovskites are known to undergo photoinduced and laser-induced degradation resulting in phase segregations. Udalova *et al.* demonstrated the photochemical degradation of hybrid lead iodide perovskites upon laser irradiation, resulting in polyiodides.[12] In the case of HDPs, to the best of our knowledge, such studies are scarce. However, we believe it is quite possible that the laser-induced degradation could play a significant role in converting the phase locally. To understand whether the degradation is induced by a thermal effect or due to a laser light exposure effect, Raman spectra of $Cs_2AgBiBr_6$ are acquired using a high laser power. At temperatures below 180 °C, all the Raman spectra are identical when the spectra were acquired with lower power excitation. However, at temperatures above 180 °C, we observe that the Raman modes get altered with the emergence of several new peaks (marked with the symbol *). This indicates the structural degradation of $Cs_2AgBiBr_6$ and the formation of a new phase, *viz.* $Cs_3Bi_2Br_9$. The F_{2g} mode at 74.8 cm^{-1} splits into three peaks ($2E_g$ and $1A_{1g}$), which can be attributed to the vibrations associated with $BiBr_6$ octahedra involving only Br atoms.[17] One of the three low energy peaks ($1E_g$) corresponds to the octahedral vibrations around the x, y axes. The other two peaks could be due to the deformational vibrations of $BiBr_6$ octahedra.[17] This indicates a deformation of the cubic lattice. The intense A_{1g} mode of $Cs_2AgBiBr_6$ at ~177.5 cm^{-1}, which is observed at all temperatures for low laser power excitation or at temperatures below 180 °C for high power laser excitation, disappears and two new peaks at ~161 cm^{-1} and ~185 cm^{-1} emerge at temperatures >180 °C upon excitation with a 7.15 mW, 632 nm laser source. These two modes are A_{1g} (~161 cm^{-1}) and E_g (~185 cm^{-1}) vibrations arising from the stretching of Bi–Br bonds in the $Cs_3Bi_2Br_9$ structure.[17] Thus, it is evident from our Raman spectral studies that the $Cs_2AgBiBr_6$ phase degrades to $Cs_3Bi_2Br_9$ only upon using a high laser power. This is in stark contrast to an earlier report by Pistor *et al.*, in which $Cs_2AgBiBr_6$ is found to be thermally stable only up to 250 °C.[9] Our study unequivocally demonstrates that (i) $Cs_2AgBiBr_6$ is stable up to high temperatures of 410 °C, as discussed in the following section, and (ii) $Cs_2AgBiBr_6$ can degrade under the influence of an intense laser source. The degradation does not happen at lower temperatures (<180 °C) as the compound is inherently stable, whereas, at higher temperatures, higher laser intensities generate a significant amount of localized heat resulting in the local degradation of $Cs_2AgBiBr_6$.

It is known that the intense laser irradiation on samples would increase the local temperature, which would cause thermal decomposition of the compounds.[18] The increase in temperature upon laser exposure can be estimated[19] and in the present case a rough estimate is expected to be around a few hundred Kelvin. As the sample temperature is raised using an external heater, the net temperature can go beyond the decomposition temperature locally (~420 °C) leading to the decomposition of $Cs_2AgBiBr_6$ at 180 °C in the *in situ* heating experiments. This is consistent with our observation. The Raman spectra acquired at room temperature using low power laser excitation on the compound obtained by annealing it in an air ambiance up to 410 °C shows no tendency for decomposition. On the contrary, when the same study is performed under intense high power laser illumination, in *in situ* heating experiments, the sample decomposes at 180 °C. This clearly indicates that the intense laser photons generate localized heat in the sample. This local heat in addition to the externally applied heat (~180 °C) can make the overall temperature reach beyond the decomposition temperature locally (>420 °C), thus resulting in decomposition to other phases.

To further confirm the thermal stability of the compound, we performed both static and dynamic thermogravimetry analyses (TGAs). Simultaneous TGA with differential scanning calorimetry (DSC) studies performed on $Cs_2AgBiBr_6$ powder are shown in Fig. 3. The measurements are performed in an air ambiance from 25 °C to 600 °C with a heating rate of 5 °C min^{-1}. The weight percentage and heat flow changes with temperature are plotted in Fig. 3. TGA studies show that the as-prepared $Cs_2AgBiBr_6$ powder does not undergo any weight loss until a temperature of ~410 °C. DSC studies also do not show any sharp endothermic/exothermic peaks indicating that there are no phase transformations in this temperature range. This confirms the thermal stability of $Cs_2AgBiBr_6$ up to ~410 °C. Beyond 410 °C, we observe a sharp endothermic peak at 420 °C. At this temperature, the weight loss also seems to begin. The weight loss proceeds continuously and the specimen undergoes ~35% weight loss until 600 °C. This gradual weight loss indicates that $Cs_2AgBiBr_6$ does not undergo spontaneous decomposition. This is due to the positive values of decomposition enthalpies for its decomposition pathways.[20]

We also performed XRD studies on $Cs_2AgBiBr_6$ samples annealed under static conditions in open-air at 250 °C, 410 °C, and 450 °C for 30 min to understand the phase changes that would arise upon annealing at elevated temperatures (Fig. 4). It is observed that $Cs_2AgBiBr_6$ is phase-pure with the cubic structure intact up to ~400 °C. Beyond 410 °C, $Cs_2AgBiBr_6$ decomposes, yielding other phases like $Cs_3Bi_2Br_9$ and

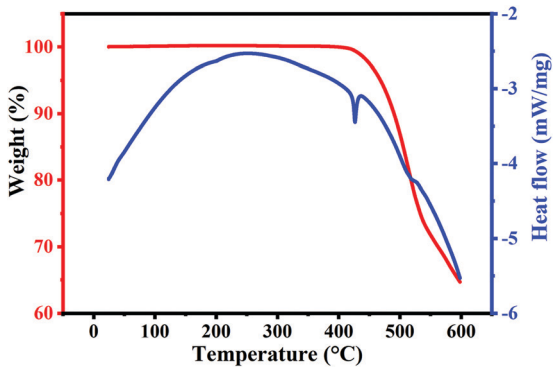

Fig. 3 DSC-TGA plots of $Cs_2AgBiBr_6$ powder in the temperature range from 25 °C to 600 °C.

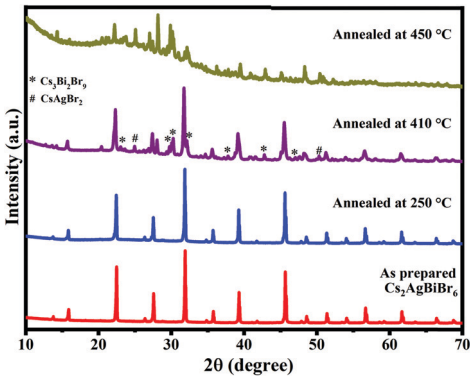

Fig. 4 XRD patterns of $Cs_2AgBiBr_6$ samples annealed at 250 °C, 410 °C, and 450 °C, along with the as-prepared sample.

$CsAgBr_2$. The XRD patterns for the sample annealed at 410 °C show intense cubic $Cs_2AgBiBr_6$ reflections along with minor secondary peaks, which correspond to $Cs_3Bi_2Br_9$ and $CsAgBr_2$.[21,22] This indicates that $Cs_2AgBiBr_6$ starts decomposition at temperatures ~410 °C, consistent with TGA-DSC studies, wherein no weight loss is seen until 410 °C. Upon further annealing at 450 °C, $Cs_2AgBiBr_6$ completely decomposes into binary and ternary bromide compounds and oxybromide compounds (Fig. 4 and 5). Thus, it is evident that the $Cs_2AgBiBr_6$ compound is thermally stable up to a much higher temperature, unlike the earlier report by Pistor *et al.*[9] Although we see the similar degradation of $Cs_2AgBiBr_6$ at 180 °C through Raman spectral analyses, it is not due to the thermal degradation of the compound as reported by Pistor *et al.*, but instead, it is laser-induced degradation of the sample at high temperatures with higher laser intensities. We have also confirmed this argument by collecting the Raman spectra of the samples annealed under static conditions at 410 °C and 450 °C (Fig. 5). The Raman spectrum of the sample annealed at 410 °C clearly shows the Raman modes of $Cs_2AgBiBr_6$ without any trace of Raman peaks from other phases. This strongly suggests that the cubic perovskite structure is intact up to 410 °C. The spectra collected for the sample annealed at 450 °C were found to be highly inhomogeneous, showing a different set of peaks at different regions. These were mostly from $Cs_3Bi_2Br_9$, Cs_3BiBr_6, and other possible oxybromides, including BiOBr. This definitely shows the thermal degradation of the sample around 450 °C.

Furthermore, we have tried to synthesize the decomposition products like $Cs_3Bi_2Br_9$, Cs_3BiBr_6, BiOBr and $CsAgBr_2$ in phase-pure forms. $Cs_3Bi_2Br_9$ and BiOBr compounds can be synthesized with phase purity as evident from the XRD and Raman studies (Fig. S1 and S2, ESI†). Phase-pure synthesis of Cs_3BiBr_6 is challenging and the solution-based synthesis of the Cs_3BiBr_6 compound resulted in a mixture of phases like $Cs_3Bi_2Br_9$ and Cs_3BiBr_6 as observed from the Raman studies. Furthermore, the $CsAgBr_2$ compound did not form when synthesized *via* a

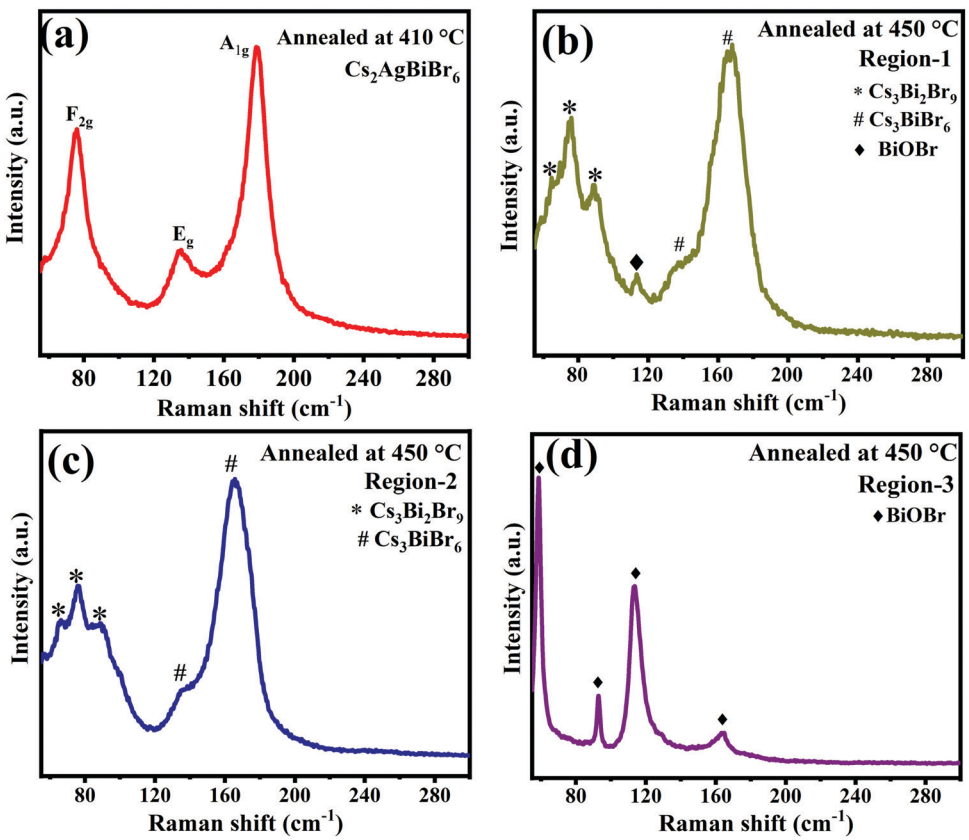

Fig. 5 Raman spectra of $Cs_2AgBiBr_6$ annealed at (a) 410 °C, and 450 °C (b, c and d) at different regions.

solution-based approach. We tried to synthesize $CsAgBr_2$ through a solid-state reaction by thoroughly grinding equimolar concentrations of CsBr and AgBr, followed by annealing. The obtained compound shows diffraction peaks corresponding to orthorhombic $CsAgBr_2$ along with some unidentifiable minor phases and agrees with the reported literature.[23] The XRD and Raman spectra for all these compounds are acquired under the same conditions that are employed for $Cs_2AgBiBr_6$. The diffraction patterns and the spectra found in the decomposition products are in good agreement with the compounds synthesized individually (Fig. S1 and S2, ESI†). This further substantiates the origin of extra peaks and the assignment of the decomposition byproducts.

4. Conclusions

In summary, thermal stability and photostability studies are performed on the $Cs_2AgBiBr_6$ compound using temperature-dependent Raman spectra and TGA-DSC studies. $Cs_2AgBiBr_6$ is thermally stable up to $\sim$410 °C. However, in the presence of a high-intensity laser power source, the stability of the compound comes down to 180 °C. This could be due to the localized heating arising from intense laser light resulting in local decomposition. This study, thus, unequivocally shows the photoinduced thermal instability in an otherwise thermally stable compound. We believe such a study on this novel compound is the first of its kind and will be of great utility to effectively integrate $Cs_2AgBiBr_6$ into various optoelectronic devices.

Conflicts of interest

There are no conflicts to declare.

Acknowledgements

C. S. acknowledges the Ministry of Education, Government of India, for funding this work through Scheme for Transformational and Advanced Research in Sciences (STARS) vide STARS/APR2019/NS/537/FS. C. S. acknowledges the support by MHRD, India through the Institutes of Eminence (vide SP20210777DRMHRDDIRIIT) for the research initiatives on establishing the prospective Centre for Advanced Microscopy and Materials (vide SB20210844MMMHRD008277).

References

1 F. Igbari, Z.-K. Wang and L.-S. Liao, *Adv. Energy Mater.*, 2019, **9**, 1803150.
2 P.-K. Kung, M.-H. Li, P.-Y. Lin, J.-Y. Jhang, M. Pantaler, D. C. Lupascu, G. Grancini and P. Chen, *Sol. RRL*, 2020, **4**, 1900306.
3 X. Yang, W. Wang, R. Ran, W. Zhou and Z. Shao, *Energy Fuels*, 2020, **34**, 10513–10528.
4 R. L.-Z. Hoye, L. Eyre, F. Wei, F. Brivio, A. Sadhanala, S. Sun, W. Li, K. H.-L. Zhang, J. L. MacManus-Driscoll, P. D. Bristowe, R. H. Friend, A. K. Cheetham and F. Deschler, *Adv. Mater. Interfaces*, 2018, **5**, 1800464.
5 D. Bartesaghi, A. H. Slavney, M. C. Gélvez-Rueda, B. A. Connor, F. C. Grozema, H. I. Karunadasa and T. J. Savenije, *J. Phys. Chem. C*, 2018, **122**, 4809–4816.
6 F. Ji, J. Klarbring, F. Wang, W. Ning, L. Wang, C. Yin, J. S.-M. Figueroa, C. K. Christensen, M. Etter, T. Ederth, L. Sun, S. I. Simak, I. A. Abrikosov and F. Gao, *Angew. Chem., Int. Ed.*, 2020, **59**, 15191–15194.
7 B. Wang, N. Li, L. Yang, C. Dall'Agnese, A. K. Jena, S. Sasaki, T. Miyasaka, H. Tamiaki and X. Wang, *J. Am. Chem. Soc.*, 2021, **143**(5), 2207–2211.
8 T. Burwig, M. Guc, V. Izquierdo-Roca and P. Pistor, *J. Phys. Chem. C*, 2020, **124**, 9249–9255.
9 P. Pistor, M. Meyns, M. Guc, H.-C. Wang, M. A.-L. Marques, X. Alcobé, A. Cabot and V. Izquierdo-Roca, *Scr. Mater.*, 2020, **184**, 24–29.
10 M. Ghasemi, L. Zhang, J.-H. Yun, M. Hao, D. He, P. Chen, Y. Bai, T. Lin, M. Xiao, A. Du, M. Lyu and L. Wang, *Adv. Funct. Mater.*, 2020, **30**, 2002342.
11 Y.-C. Qiao, Y.-H. Wei, Y. Pang, Y.-X. Li, D.-Y. Wang, Y.-T. Li, N.-Q. Deng, X.-F. Wang, H.-N. Zhang, Q. Wang, Z. Yang, L.-Q. Tao, H. Tian, Y. Yang and T.-L. Ren, *Jpn. J. Appl. Phys.*, 2018, **57**, 04FA01.
12 N. N. Udalova, A. S. Tutantsev, Q. Chen, A. Kraskov, E. A. Goodilin and A. B. Tarasov, *ACS Appl. Mater. Interfaces*, 2020, **12**, 12755–12762.
13 C. Wu, B. Du, W. Luo, Y. Liu, T. Li, D. Wang, X. Guo, H. Ting, Z. Fang, S. Wang, Z. Chen, Y. Chen and L. Xiao, *Adv. Opt. Mater.*, 2018, **6**, 1800811.
14 W. Yuan, G. Niu, Y. Xian, H. Wu, H. Wang, H. Yin, P. Liu, W. Li and J. Fan, *Adv. Funct. Mater.*, 2019, **29**, 1900234.
15 A. C. Dakshinamurthy and C. Sudakar, *J. Phys. Chem. Lett.*, 2022, **13**, 433–439.
16 A. C. Dakshinamurthy and C. Sudakar, *Appl. Phys. Lett.*, 2021, **118**, 131902.
17 M. Y. Valakh, M. P. Lisitsa, E. Y. Peresh, O. V. Trylis and A. M. Yaremko, *J. Mol. Struct.*, 1997, **436-437**, 309–313.
18 L. Han, M. Zeman and A. H.-M. Smets, *Nanoscale*, 2015, **7**, 8389–8397.
19 B. H. Venkataraman, N. S. Prasad, K. B.-R. Varma, V. Rodriguez, M. Maglione, R. Vondermuhll and J. Etourneau, *Appl. Phys. Lett.*, 2005, **87**, 091113.
20 Z. Xiao, W. Meng, J. Wang and Y. Yan, *ChemSusChem*, 2016, **9**, 2628–2633.
21 J. Su, Y.-q Huang, H. Chen and J. Huang, *Cryst. Res. Technol.*, 2020, **55**, 1900222.
22 M. N. Tran, I. J. Cleveland and E. S. Aydil, *J. Mater. Chem. C*, 2020, **8**, 10456–10463.
23 Z. Zhang, R. Zhao, S. Teng, K. Huang, L. Zhang, D. Wang, W. Yang, R. Xie and N. Pradhan, *Small*, 2020, **16**, 2004272.